ELSEVIER

Journal of Wind Engineering
and Industrial Aerodynamics 91 (2003) 101–111

JOURNAL OF
wind engineering
AND
industrial
aerodynamics

www.elsevier.com/locate/jweia

Effects of oscillation amplitude on aerodynamic derivatives

M. Noda*, H. Utsunomiya, F. Nagao, M. Kanda, N. Shiraishi

Department of Civil Engineering, Faculty of Engineering, University of Tokushima, 2-1, Minami-Josanjima, Tokushima 770-8506, Japan

Abstract

In this paper, the effects of oscillation amplitude on the aerodynamic derivatives of the thin rectangular cylinder with $B/D = 13$ and 150 were investigated. It was clear that the torsional amplitude affected strongly the aerodynamic derivatives H_2^* and A_2^*. This effect reduced the critical velocity of flutter by about 10%. The cause of this effect was investigated by the measurement of the unsteady surface pressure. This investigation made it clear that the variation of A_2^* is caused by the movement of the acting point of the resultant lift force. These results indicate that these effects cannot be disregarded for such a simple thin plate but for a real bridge girder with a more complex cross-section and with delicate aerodynamic control devices.

Keywords: Aerodynamic derivatives; Torsional flutter; Effects of oscillating amplitude; Experimental condition

1. Introduction

In order to evaluate the safety of a long span bridge against flutter instability problems, it is very important to understand the aerodynamic derivatives of its bridge deck accurately. Usually, the flutter analysis is carried out with the aerodynamic derivatives obtained by wind tunnel experiment with scaled model of bridge deck. However, it is well known that the aerodynamic derivatives depend on the experimental conditions such as the reduced wind speed, amplitude of forced oscillation and wind properties [1]. In order to confirm the stability against any flutters accurately, it is also important to understand the effects of experimental

*Corresponding author. Tel.: +81-88-656-7323.
E-mail address: tarda@ce.tokushima-u.ac.jp (M. Noda).

0167-6105/02/$ - see front matter
PII: S0167-6105(02)00338-0

conditions on the aerodynamic derivatives. Especially, after conducting a wind tunnel experiment, there is no standard to determine the conditions of the oscillating amplitude.

In this paper, the effects of oscillating amplitude on the aerodynamic derivatives defined by Scanlan [2] were investigated by using a thin rectangular cylinder.

2. Experimental procedures

The wind tunnel used in this study was a semi-closed circuit type. Its working section was 1.5 m high, 0.7 m wide and 2.5 m long.

Fig. 1 shows the cross-section of test models. The slenderness ratios, B/D (the ratio of width, B, to depth, D) were 13 and 150. Two models with the same B/D and different sizes were prepared. One model, which is called Large Model was 20 mm deep and 260 mm wide, and another one called Small Model, was 5.5 mm deep and 71.5 mm wide. In addition to the measurement with load cells, surface pressure was measured with the two-dimensional model to understand the effect of amplitude on unsteady aerodynamic pressure in the case of torsional mode. This model was 23.1 mm deep and 300 mm wide. 15 pressure taps were holed on the side surface of this model. The model with $B/D = 150$ was used to measure the aerodynamic derivatives, and they were compared with theoretical results to examine the accuracy of aerodynamic force measurements. This model was 2 mm deep and 300 mm wide.

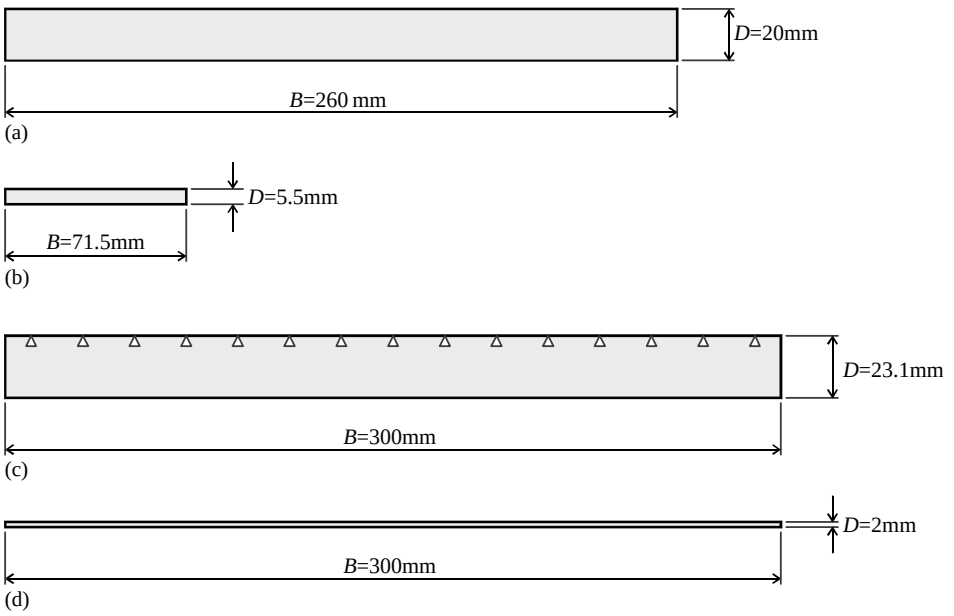

Fig. 1. Cross-section of test model: (a) $B/D = 13$ (large model); (b) $B/D = 13$ (small model); (c) $B/D = 13$ (pressure model); (d) $B/D = 150$.

The test model was oscillated forcibly in one degree of freedom, bending mode and torsional mode. In the case of $B/D = 13$, bending amplitude, η_0/D, was changed in the range 0.25–1.25. In the case of $B/D = 150$, η_0/D was changed in the range 2.5–12.5. Torsional amplitude, ϕ_0, was changed in the range 1.3°–12.2° for each model.

The aerodynamic forces exerted on these models were measured by load cells fixed on the forced oscillating system. These aerodynamic forces gave the aerodynamic derivatives defined by Matsumoto et al. [3] through the following expressions:

$$L = \frac{1}{2}\rho(2b)U^2\left\{kH_1^*\frac{\dot{\eta}}{U} + kH_2^*\frac{b\dot{\phi}}{U} + k^2H_3^*\phi + k^2H_4^*\frac{\eta}{b}\right\}, \tag{1}$$

$$M = \frac{1}{2}\rho(2b^2)U^2\left\{kA_1^*\frac{\dot{\eta}}{U} + kA_2^*\frac{b\dot{\phi}}{U} + k^2A_3^*\phi + k^2A_4^*\frac{\eta}{b}\right\}. \tag{2}$$

3. Results and discussion

3.1. Aerodynamic coefficient of the test model

Fig. 2 shows the lift coefficient, C_L, and the moment coefficient, C_M for $B/D = 13$ and 150. In the case of $B/D = 13$, the lift coefficient and the moment coefficient change linearly in the angle range of –4° to 4°. This result indicates that the stall angle for $B/D = 13$ is about 4°. On the other hand, the lift coefficient and the moment coefficient of $B/D = 150$ change linearly in the angle range of –6° to 6°. This figure shows that the stall angle for $B/D = 150$ is about 6°.

3.2. Effects of bending amplitude on aerodynamic derivatives

Fig. 3 shows the aerodynamic derivatives, H_1^*, H_4^*, A_1^*, A_4^*, obtained by bending oscillation for $B/D = 13$ and 150, respectively. The solid lines in this figure indicate the theoretical aerodynamic derivatives for a thin plate.

In this figure, H_4^* and A_4^* seem to be affected by the oscillating amplitudes and they are not consistent with the theoretical results. However, these derivatives have little effect on the flutter speed of the analysis. Another two aerodynamic derivatives, H_1^* and A_1^* change little. These results indicate that the bending amplitude has little effect on the flutter analysis of the model.

3.3. Effects of torsional amplitude on aerodynamic derivatives

Fig. 4 shows the aerodynamic derivatives, H_2^*, H_3^*, A_2^*, A_3^*, obtained by torsional oscillation for $B/D = 13$ and 150, respectively. It is found that the H_2^* and A_2^*, which are proportional to the velocity of the oscillation, are strongly affected by torsional amplitude. The variation of H_2^* with the increase of torsional amplitude for $B/D = 150$ is larger than that of $B/D = 13$. Moreover, A_2^* changed from a negative value to positive value with the increase of torsional amplitude at both B/D. The angles of

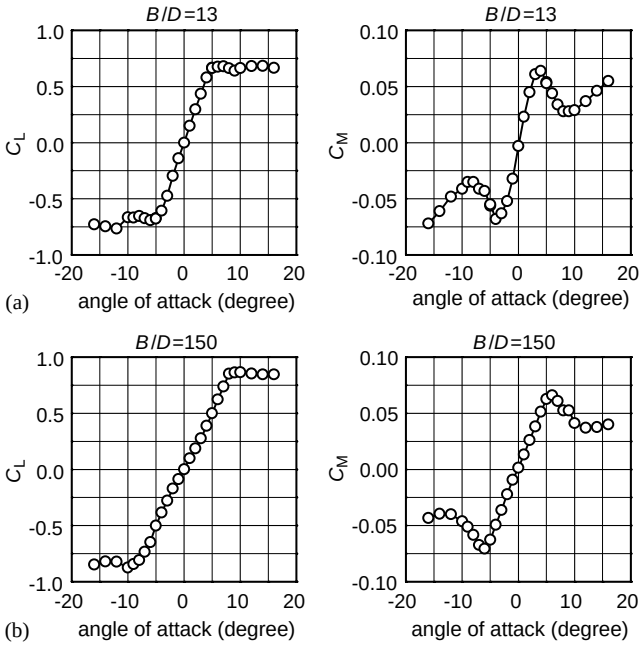

Fig. 2. Aerodynamic force coefficients: (a) $B/D = 13$; (b) $B/D = 150$.

attack with the largest A_2^* variation were about 5° for $B/D = 13$, and about 8° for $B/D = 150$. The variation of A_2^* for $B/D = 13$ is larger than that for $B/D = 150$. These results are probably related to the stall angle indicated at Fig. 3. This result suggests that the increase of torsional amplitude cause the decrease of the flutter stability in torsional mode for both B/D. In this paper, the variation of A_2^* are paid attention.

3.4. Blockage effects on aerodynamic derivatives

In this wind tunnel test, the blockage effect was examined in torsional mode of oscillation because the blockage ratio at the maximum amplitude of oscillation, S/C, became 3.7% for $B/D = 13$, where S is the ratio of projected model area and C is test section area of wind tunnel.

Therefore, to judge whether the aerodynamic derivatives were influenced by blockage ratio or not, the small model which is a quarter size of the large model, was tested for the same torsional amplitude of large model. Fig. 5 shows the test result for the small model. In this figure, it is found that the aerodynamic derivatives at the same torsional amplitude are almost the same. This result indicates that the variation of A_2^* is not caused by blockage effect, but is caused by the change of torsional amplitude.

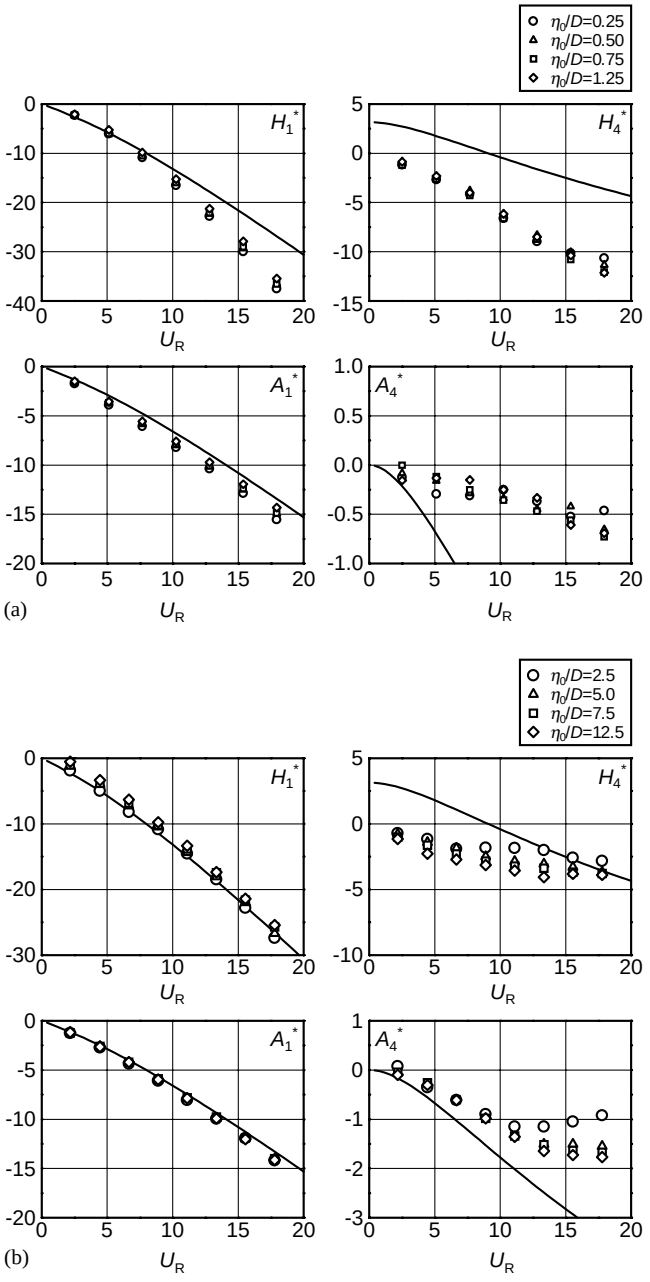

Fig. 3. Effects of bending amplitude on aerodynamic derivatives: (a) $B/D = 13$; (b) $B/D = 150$.

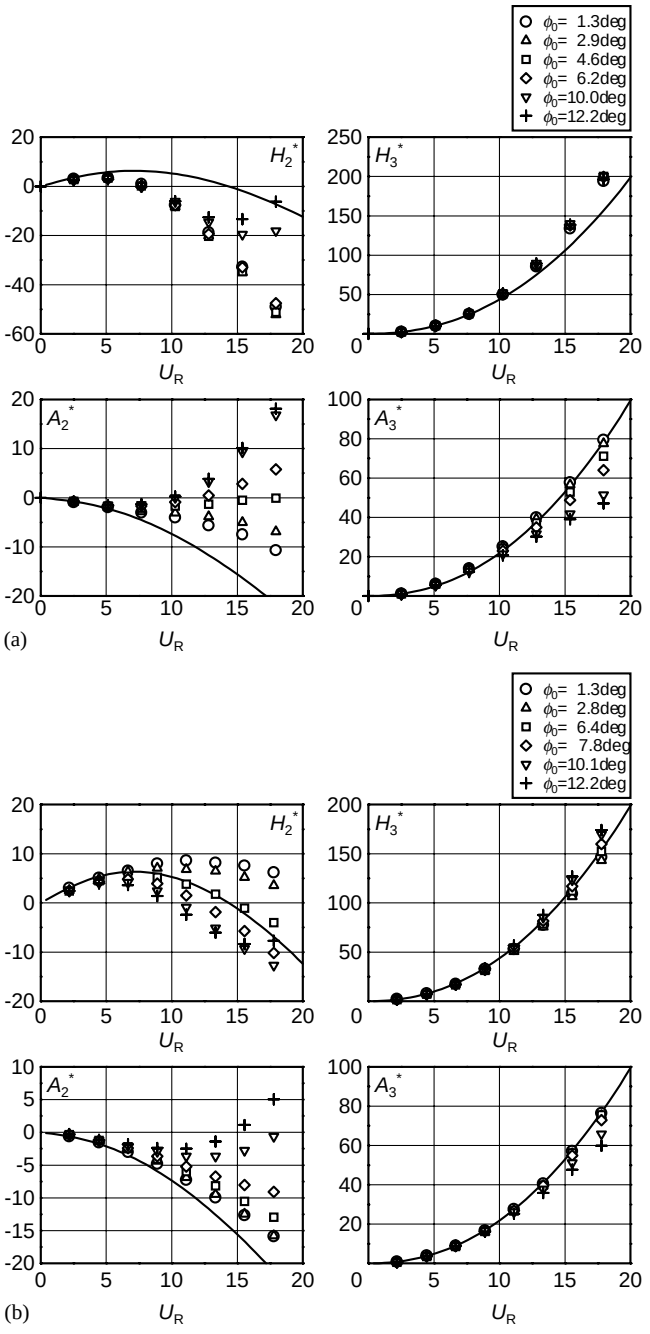

Fig. 4. Effects of torsional amplitude on aerodynamic derivatives: (a) $B/D = 13$; (b) $B/D = 150$.

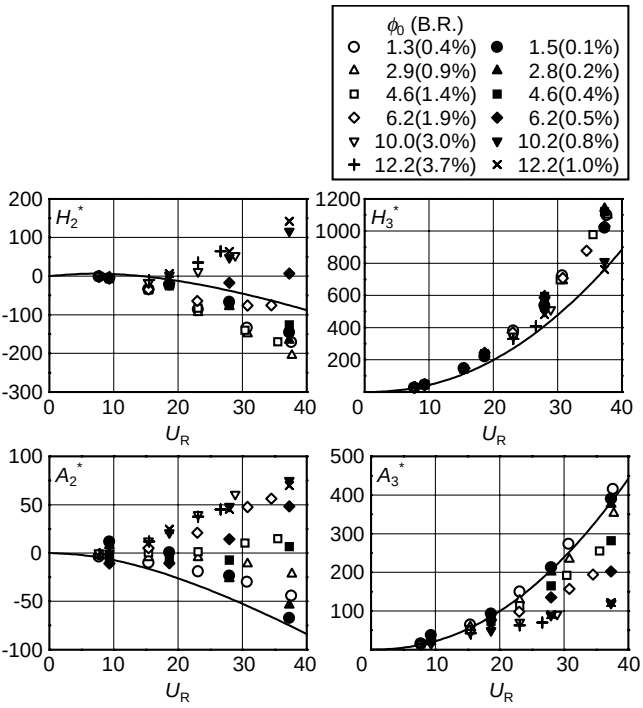

Fig. 5. Effects of blockage ratio on aerodynamic derivatives ($B/D = 13$).

3.5. Effects of the oscillation amplitude on the flutter analysis

Fig. 6 shows the results of flutter analyses by the aerodynamic derivatives shown in Figs. 3 and 4. The structural parameters on these analyses are shown in Table 1.

In Fig. 6, the critical velocity, V_{cr}, is the zero-cross point of the logarithmic decrement, δ. The upper graphs indicate the relation between velocity, V, and δ, given by different bending amplitude and the lower graphs show the $V - \delta$ relation given by different torsional amplitude. It is found that there is no change in the case of changing the bending amplitude for both B/D. On the other hand, in the case of changing the torsional amplitude, the critical velocity decreases with the increase of torsional amplitude for both B/D. The critical velocities for $B/D = 13$ and 150 were reduced by about 7% and 10%, respectively. The effects of torsional oscillating amplitude on flutter speed can be seen clearly.

3.6. Estimation on the cause of the variation of A_2^* with changing torsional amplitude

In this section, why the A_2^* depends on the change of the torsional amplitude is discussed. Fig. 7 shows the distribution of instantaneous surface pressures of $B/D = 13$ in the cases where the torsional amplitudes are 1.3° and 10.0°, respectively. The

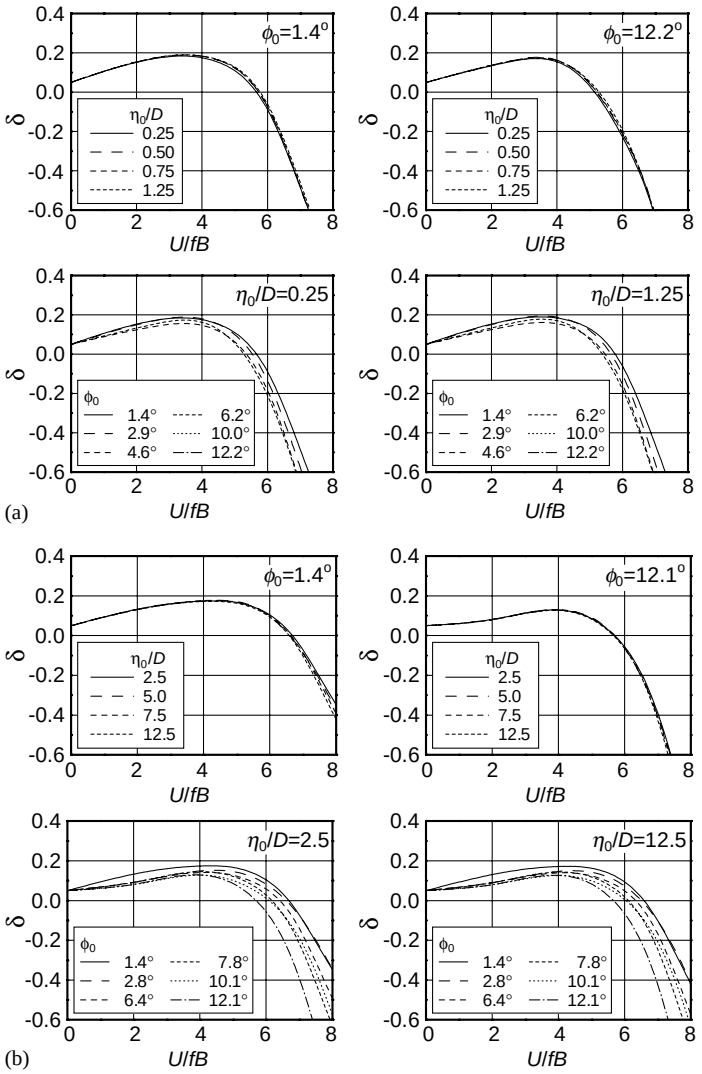

Fig. 6. Results of flutter analysis: (a) $B/D = 13$; (b) $B/D = 150$.

Table 1
Structural parameters supposed on flutter analysis

Mass	40,140 kg/m
Mass moment of inertia	7,060,900 kg m^2/m
Vertical frequency	0.0625 Hz
Torsional frequency	0.180 Hz
Vertical logarithmic decrement	0.05
Torsional logarithmic decrement	0.05

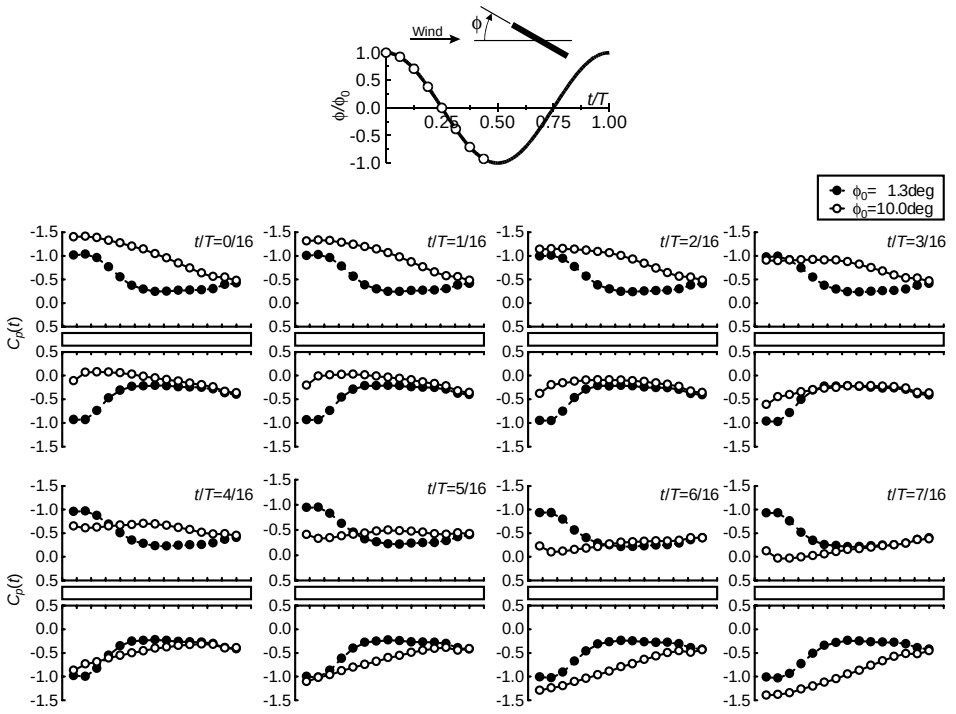

Fig. 7. Pressure fluctuations on torsional oscillation ($B/D = 13$, $U/fB = 15$).

reduced wind speed for each case is about 15. In this figure, the torsional displacement, $\phi(t)$ is given by

$$\phi(t) = \phi_0 \cos\left(2\pi \frac{t}{T}\right), \tag{3}$$

where T is the period of the oscillation.

In the case that the torsional amplitude is 1.3°, it is found that each separated flow reattaches completely at the point at a distance of about $4D$ from the leading edge. On the other hand, in the case in which the torsional amplitude is 10.0° and the reattaching point of separation flow is moving in the wide range from leading edge to trailing edge approximately, the surface pressure fluctuation is strong.

Fig. 8 shows the mean and unsteady pressure coefficient distributions for each torsional amplitude. The reduced wind speed is about 15 in all cases. This figure shows that the mean reattaching point is shifted to down-stream region and the moving range of the reattaching point becomes wide with increase of torsional amplitude.

To consider the cause of A_2^* variation, Fig. 9 shows the fluctuation of lift and moment during one cycle for each torsional amplitude. The reduced wind speed for each case is about 15. x_A in this figure is the distance from the leading edge to the

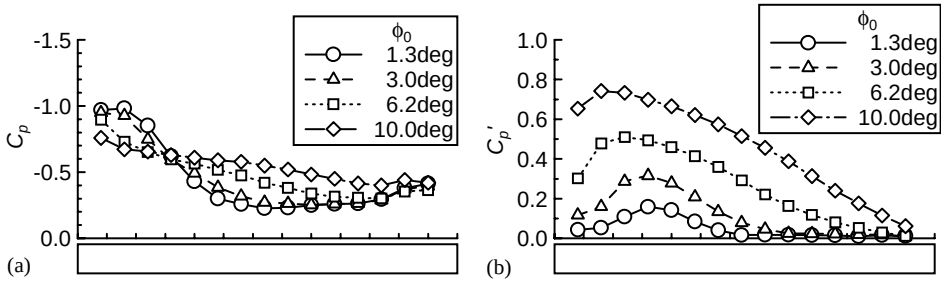

Fig. 8. Mean pressure coefficient and unsteady pressure coefficient ($B/D = 13$, $U/fB = 15$): (a) mean pressure coefficient; (b) unsteady pressure coefficient.

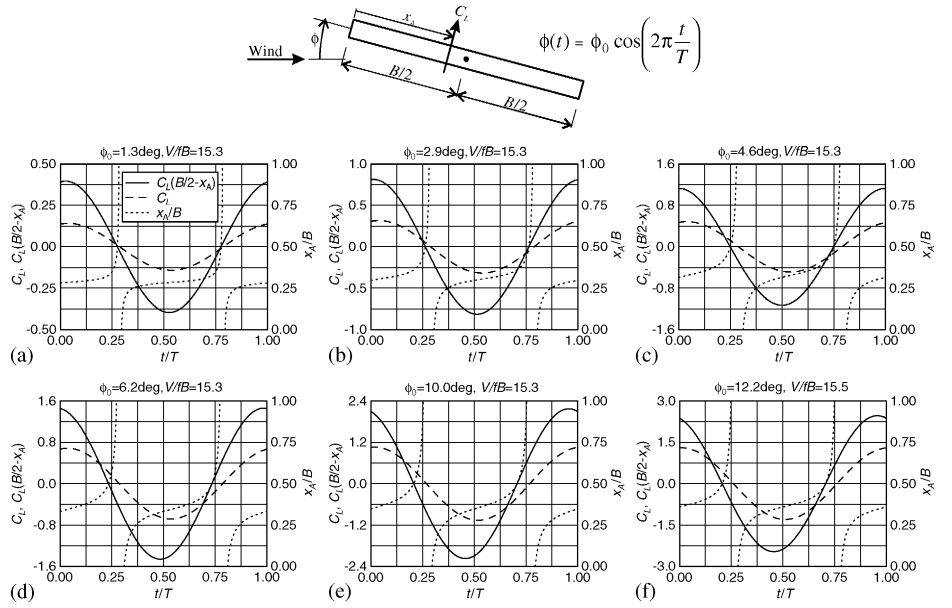

Fig. 9. The relation among lift, moment and the acting position of lift ($B/D = 13$, $U/fB = 15$): (a) $\phi_0 = 1.3°$; (b) $\phi_0 = 2.9°$; (c) $\phi_0 = 4.6°$; (d) $\phi_0 = 6.2°$; (e) $\phi_0 = 10.0°$; (f) $\phi_0 = 12.2°$.

acting point of resultant lift force. In the case $x_A/B < 0.5$, the resultant lift force acts in the up-stream region from the center of rotation.

In these figures, when the downward velocity of the oscillation is the maximum at $t/T = 0.25$, the moment changes from positive value to negative value around the torsional amplitude, 6°. It is found that the changing sign of moment is not caused by the sign of lift force, but is caused by the movement of the acting point of resultant lift force. Therefore the switching of A_2^* sign is caused by moving the acting point of resultant lift force by crossing over the center of rotation. This phenomenon looks like the process of the torsional flutter occurrence explained by Matsumoto [4].

In this process, the movement of the acting point of resultant lift force is caused by changing the slenderness ratio, B/D. In this study, the movement of the acting point of resultant lift force occurs by changing the torsional amplitude.

These results indicate that the aerodynamic derivatives are strongly affected by torsional amplitude, and its effects cannot be disregarded for such a simple thin plate but for a real bridge girder with more complex cross-section and with delicate aerodynamic control devices.

4. Conclusion

This paper discussed the effects of oscillating amplitude on the aerodynamic derivatives of the thin rectangular cylinder, with B/D 13 or 150. As the result, it was clearly seen that the torsional amplitude affected A_2^* strongly, and this effect was caused by the movement of the reattaching point of separation flow. In the case $B/D = 13$ or 150, large amplitude was needed to make the stable aerodynamic derivatives become unstable. However, the point of this study is the fact that some cross-sections with stable aerodynamic derivatives for small oscillating amplitudes become unstable for large oscillating amplitude. This result indicates the possibility that cross-section with stable aerodynamic derivatives around almost zero amplitude, which have an unstable limit cycle for the small amplitude, may become unstable by a little increase of the initial amplitude.

Therefore, we cannot predict accurately the flutter onset velocity for the cross-section that the hard flutter occurs on it, without consideration of the amplitude dependence of the aerodynamic derivatives. The standard about the oscillating amplitude will be needed to secure the safety against any flutter, followed by feature studies with more detailed and extended discussion for a real bridge cross-section.

References

[1] F. Nagao, H. Utsunomiya, M. Noda, M. Kanda, A. Ikeuchi, N. Kanaumi, Effects of experimental conditions on aerodynamic derivatives of fundamental bluff bodies, Proceedings of the Fourth International Colloquium on Bluff Body Aerodynamics and Applications, 2000.

[2] R.H. Scanlan, J.J. Tomko, Airfoil and Bridge Deck Flutter Derivatives, J. ASCE EM6 (1971).

[3] M. Matsumoto, Y. Kobayashi, Y. Niihara, M. Shirato, H. Hamasaki, Flutter mechanism and its stabilization of bluff bodies, Proceedings of the Ninth International Conference on Wind Engineering, 1995.

[4] M. Matsumoto, Torsional flutter of bluff bodies, Proceedings of the Third International Colloquium on Bluff Body Aerodynamics and Applications, 1996.